Bellcomm

955 L'Enfant Plaza North, S.W.
Washington, D. C. 20024

date: February 28, 1972

to: Distribution

B72 02012

from: R. C. Purkey

subject: Long Term Trajectory Generation with VARPAR - Case 610

## ABSTRACT

The long term trajectory generation program VARPAR was obtained from Bell Telephone Laboratories in order to determine its possible use in Skylab mission analysis. This program was found to be able to generate a 240-day Skylab trajectory in thirty seconds of CPU time on the UNIVAC 1108 computer. VARPAR trajectories were compared to actual satellite histories and found to have a maximum error of 117° in mean anomaly after 270 days, which is well within the dispersion to be expected due to drag. Trajectories generated by MSC and MSFC were also compared to VARPAR trajectories. Here the uncertainty due to drag was ostensibly eliminated by using equivalent drag models and data. These MSC and MSFC trajectories differed in argument of latitude by a maximum of 0.6° and 51° respectively after 29 days of propagation.

Bellcomm

955 L'Enfant Plaza North, S.W.
Washington, D. C. 20024

date: February 28, 1972

to: Distribution

B72 02012

from: R. C. Purkey

subject: Long Term Trajectory Generation with VARPAR - Case 610

MEMORANDUM FOR FILE

## Introduction

Mission analysis for Skylab requires the need of a trajectory generator which can compute a very accurate trajectory over periods of time up to 240 days. It should also be able to generate these trajectories in a minimum of computer time, in order that it may be used effectively in mission planning iterations. Bellcomm currently uses a program known as BCMASP to generate these orbital trajectories. This program uses standard methods of numerical integration to propagate the position and velocity vector of a satellite. While this method is accurate for many purposes, it is extremely slow and requires an enormous amount of computer time to generate a 240-day trajectory. Therefore, a study of the available literature was undertaken in search of a better technique for propagating a satellite state in earth orbit.

During this investigation it became apparent that most high speed orbit propagation techniques work with some form of mean orbital elements generally related to Keplerian osculating conic elements. Translation between these mean elements and instantaneous position and velocity vectors generally appeared difficult and often ill-defined -- a handicap because we required input and output to be in this form. An exception was the technique described in References 1 and 2 wherein osculating conic elements are directly propagated. Translation to and from instantaneous position and velocity vectors is relatively straightforward and can be done with well known standard equations. This technique had been developed at the Bell Telephone Laboratories (BTL), named VARPAR, and was claimed to feature a high degree of accuracy over long terms of propagation and extremely fast orbit propagation. The technique had been coded into working computer routines and Mr. George J. Miron of BTL obligingly supplied us with card decks and documentation. The programs were converted for use on the UNIVAC 1108, checked out, and then numerous comparison studies were performed.

VARPAR

VARPAR is a trajectory generation program which propagates the osculating conic elements of a satellite's orbit from one ascending node to the next. The orbital elements generated are: semi-major axis (a), inclination (i), right ascension of the ascending node ($\Omega$), eccentricity multiplied by the sine of the argument of perigee (m), eccentricity multiplied by the cosine of the argument of perigee (l), and the time of pseudo-nodal passage, $T=\tau-\omega/\eta$ (where $\tau$ is the time of perigee passage, $\omega$ is the argument of perigee, the mean motion $\eta = \sqrt{\mu/a^3}$ with $\mu$ the gravitational constant of the earth). This set of orbital elements is valid for both circular and elliptical orbits.

The equations evaluated by VARPAR were derived by integrating Lagrange's planetary equations by analytic quadratures. The independent variable in this integration was the argument of latitude. This integral was evaluated between 0 and $2\pi$ radians to yield what is defined as secular changes in the elements from one node to the next. This definition of secular changes combines the effects of both the long term periodic and the secular changes that some other authors define. Short period variations are omitted, since by definition their integral is identically zero over each full revolution. The equations account for orbit perturbations due to the earth's oblateness by considering the first 14 zonal harmonics of the geopotential. These closed form equations are valid for all non-equatorial orbits, including those at the so-called critical inclination. The effects of atmospheric drag and solar and lunar gravitation were also derived as closed form equations. Together, these equations yield a highly accurate evaluation of the secular variation in the orbital elements in traveling from ascending node to ascending node.

Simplified equations are also included to get the elements at some intermediate time between nodal crossings. These equations assume the secular changes continue linearly over the orbit, and add the strong short-period perturbation due to $J_2$, the principal earth oblateness term. While there is an intrinsic error in omitting higher order effects, the error magnitude remains small because the simplified equations are only used up to 360° of motion. Although VARPAR can go from a node to an intermediate point, it cannot do the reverse; the trajectory must be initialized at an ascending node. This ensures that the highly accurate node-to-node propagation is not inadvertently corrupted by erroneous initial data, and puts the burden on the user to provide suitably precise initial values at a node.

The drag perturbation equations in VARPAR assume an atmosphere of the form:

$$\rho = \rho_o e^{(\beta_o + \beta_1/R)} = \rho_o e^{\frac{-\beta h}{1 + \frac{h}{R_e}}} \qquad (1)$$

where $\rho$ is the atmospheric density, $\rho_o$, $\beta_o$, and $\beta_1$ are constants and R is the geocentric distance to the vehicle. In the alternate form, h is altitude above a spherical earth of radius $R_e$ and $\beta$ is an empirical constant. This expression was originally selected because it rather accurately matched the 1962 U.S. Standard atmospheric density model over an altitude range of several hundred thousand feet. The expression is less successful in fitting the Jacchia atmospheric density model in that the region of good agreement shrinks to one-tenth the previous size. However, for near circular orbits like the Skylab, this limited region of agreement presents no problem.

Equation (1), which defines the atmospheric density, was used to develop the analytic expressions for the changes to the orbital elements. The constants $\rho_o$, $\beta_o$, and $\beta_1$ are determined outside VARPAR by fitting Equation (1) to the atmospheric density data desired. The Jacchia atmosphere model is more complicated in that it includes a bulge toward the sun and slow variations due to changes in solar activity in addition to the predominant decay versus altitude. Since Equation (1) accounts for only the altitude variation, the other factors had to be accounted for by other means. The solar bulge was eliminated by averaging the densities at a given altitude on a specific date around an orbit and for all orientations between the orbit plane and sun. Since the variation in this average density for various dates was large (due to predicted changes in solar activity), the averages were computed and fitted with Equation (1) at two-month intervals. The constants $\rho_o$, $\beta_o$, and $\beta_1$ for each date were then arranged in a table for VARPAR to reference as needed.

The analytic equations describing the changes in the orbital elements due to drag are not valid for all eccentricity - semi-major axis combinations. In fact,

$$\frac{e}{1-e^2} < \frac{12a}{\beta_1}$$

must be satisfied in order to insure convergence of the equations. For example, the Skylab orbit with a semi-major axis of 22,353,625 ft and $\beta_1$ equal $2.826 \times 10^9$ must have an eccentricity less than .095. This limit is clearly much larger than any eccentricity expected for Skylab.

Speed and Accuracy Tests

VARPAR was found to be able to generate a 240-day Skylab trajectory that consisted of the time and longitude of every ascending nodal crossing in thirty seconds of CPU time on a UNIVAC 1108 computer. This run was made with the standard version of VARPAR and included the effects of atmospheric drag and solar and lunar perturbations. The program used about 19,000 decimal words of storage. For comparison, Bellcomm's general orbital simulator (BCMASP), which numerically integrates state vectors, took over two hours of CPU time to generate a similar 240-day trajectory. With VARPAR's small storage requirement and the rapid computation speed, VARPAR will certainly be very useful since it may be used frequently.

The accuracy of VARPAR was determined by comparison with two satellite orbit element histories published by the Smithsonian Astrophysical Observatory. These mean orbital elements were computed from tracking data and are available for periods of several hundred days. Specifically, the two satellites used in the test are the 1962 $\beta\mu$ and the 1964-5A (Saturn V) (References 3, 4, 5, and 6). The 1962 $\beta\mu$ was in an orbit with a semi-major axis altitude of 609.8 nm and an eccentricity of .0076. The 1964-5A was in an orbit with a semi-major axis altitude of 273 nm and an eccentricity of .03580. The 1962-$\beta\mu$ was a test of VARPAR in the absence of drag, while the 1964-5A, with its 140 nm perigee altitude, was a test with large drag perturbations.

In order to compare the VARPAR osculating orbital elements with the Smithsonian mean elements, a computational procedure was needed to convert osculating elements to mean elements. Osculating orbital elements represent the instantaneous conic orbit while the Smithsonian mean elements are essentially osculating elements with the short period variations removed. The transformation was made by averaging the osculating elements over one nodal period, centered about the desired epoch. This had the desired effect of eliminating the short period terms in the osculating elements.

Initializing VARPAR from the Smithsonian data was computationally difficult. As stated earlier, VARPAR requires osculating orbit elements at the ascending node for initialization and converting from mean elements to osculating elements is an ill-defined process. Since the Smithsonian gives mean orbital elements at 24-hour intervals, not at the node, a multiple step conversion process was developed. This process involved the evaluation of analytic expressions (based on Kozai's work, Reference 8) to obtain an estimate of the position and velocity vectors at the given epoch. The vectors were then numerically integrated forward to the nearest ascending node where the state was converted back to the osculating elements needed to initialize VARPAR. When these osculating elements were projected by VARPAR to each of the subsequent data epochs, they matched quite well in all the elements except mean motion, where the error residuals included a linear slope and pseudo-random fluctuations. (The Smithsonian elements contain mean motion in place of semi-major axis.) Recognizing that the linear component would be caused by an erroneous semi-major axis, the initial value of this parameter was iteratively changed to eliminate the linear trend over the period of interest. The results of the test compare the eccentricity, inclination, ascending node, argument of perigee, and mean anomaly at each epoch listed by the Smithsonian.

The 1964-5A required, as input, a ballistic coefficient in order to compute the drag effects. A ballistic coefficient for this satellite of 116 $kg/m^2$ given in Reference 7 was used. The 1962 $\beta\mu$ was projected with no drag perturbations.

The results of projecting the 1962 $\beta\mu$ are shown in Figure 1. This is a plot of the error in mean anomaly versus time in days. This figure shows a maximum error of $\pm 2.0$ degrees in 360 days. The other orbital elements computed were within the stated accuracy limits of the Smithsonian data and were not plotted.

The 1964-5A results are shown in Figures 2, 3, and 4. Figure 2 shows the error in mean anomaly versus time. The mean anomaly for this satellite differs from the VARPAR solution by a maximum of 117 degrees in the 270 day period considered. Figure 3 shows the error in right ascension of the ascending node. Here the maximum error is .22°. Finally, Figure 4 shows the error in argument of perigee which, at most, is 1.2°. The other element errors were within the accuracy limits of the reference set.

The good accuracy of the prediction of the 1962 βμ satellite serves to verify VARPAR's model of the perturbations due to oblateness and solar-lunar gravitation. For the 1964-5A orbit the systematic variation in the mean anomaly residual error is probably due to an imperfect drag or atmosphere model. These same errors would occur in any other trajectory generator that uses a comparable drag model and in any case, are acceptable for use in most mission planning activities.

VARPAR was also compared with the trajectory generation programs used at MSC and MSFC. These comparisons were based on standard Skylab orbits computed with drag perturbations for a period of 29 days. Reference 9 contained the MSFC trajectory and Reference 10 the MSC trajectory. This comparison required very precise input conditions in order to make the results meaningful. Since computational difficulties are present in converting a state vector given at an arbitrary time to orbital elements at a node, the initial conditions needed for VARPAR were computed iteratively. This computation solved for the orbital elements at the node previous to the first data point of each trajectory. These initial values were iteratively changed until VARPAR produced the exact orbital elements at the first data point of each trajectory.

Figures 5, 6, and 7 show the differences between VARPAR and the MSFC trajectory for semi-major axis, argument of perigee, and argument of latitude. Figures 8, 9, and 10 show the differences between VARPAR and the MSC trajectory for the same orbital elements. The inclination, ascending node, and eccentricity differences were insignificant in both cases and, therefore, were not plotted. As can be seen in the figures, VARPAR was in close agreement with the MSC trajectory, but was not nearly so close to the MSFC trajectory.

VARPAR was also compared with a corresponding MSC Skylab trajectory computed without the drag perturbations. The differences for this 240-day projection are shown in Figures 11, 12, and 13 for the semi-major axis, argument of perigee, and argument of latitude. The differences in inclination, ascending node, and eccentricity were again negligible.

R. C. Purkey

1025-RCP-1i

Attachments

## References


1. A. J. Claus and A. G. Lubowe, A High Accuracy Perturbation Method with Direct Application to Communications Satellite Orbit Prediction, Astronautica Acta 9, p. 275-301, (1963).

2. A. G. Lubowe, High Accuracy Orbit Prediction from Node to Node, Astronautica Acta 10, p. 253-261, (1964).

3. B. Miller, Smithsonian Astrophysical Observatory Special Report 287, Satellite Orbital Data. p. 40-41.

4. B. Miller, Smithsonian Astrophysical Observatory Special Report 289, Satellite Orbital Data, p. 35-36.

5. B. Miller, Smithsonian Astrophysical Observatory Special Report 208, Satellite Orbital Data, p. 86-87.

6. B. Miller, Smithsonian Astrophysical Observatory Special Report 209, Satellite Orbital Data, p. 83-85.

7. Russell Pimm, Long-Term Orbital Trajectory Determination by Superposition of Gravity and Drag Perturbations, AAS/AIAA Astrodynamics Specialists Conference, 1971.

8. Y. Kozai, The Astronomical Journal, 64, No. 1274, November 1959, p. 367-377.

9. J. B. Haussler, Revised Skylab Orbital Trajectory Data, MSFC, S&E-AERO-MM-50-71, August 20, 1971.

10. Letter to D. A. De Graaf from John P. Mayer, MSC/MPAD, November 11, 1971.

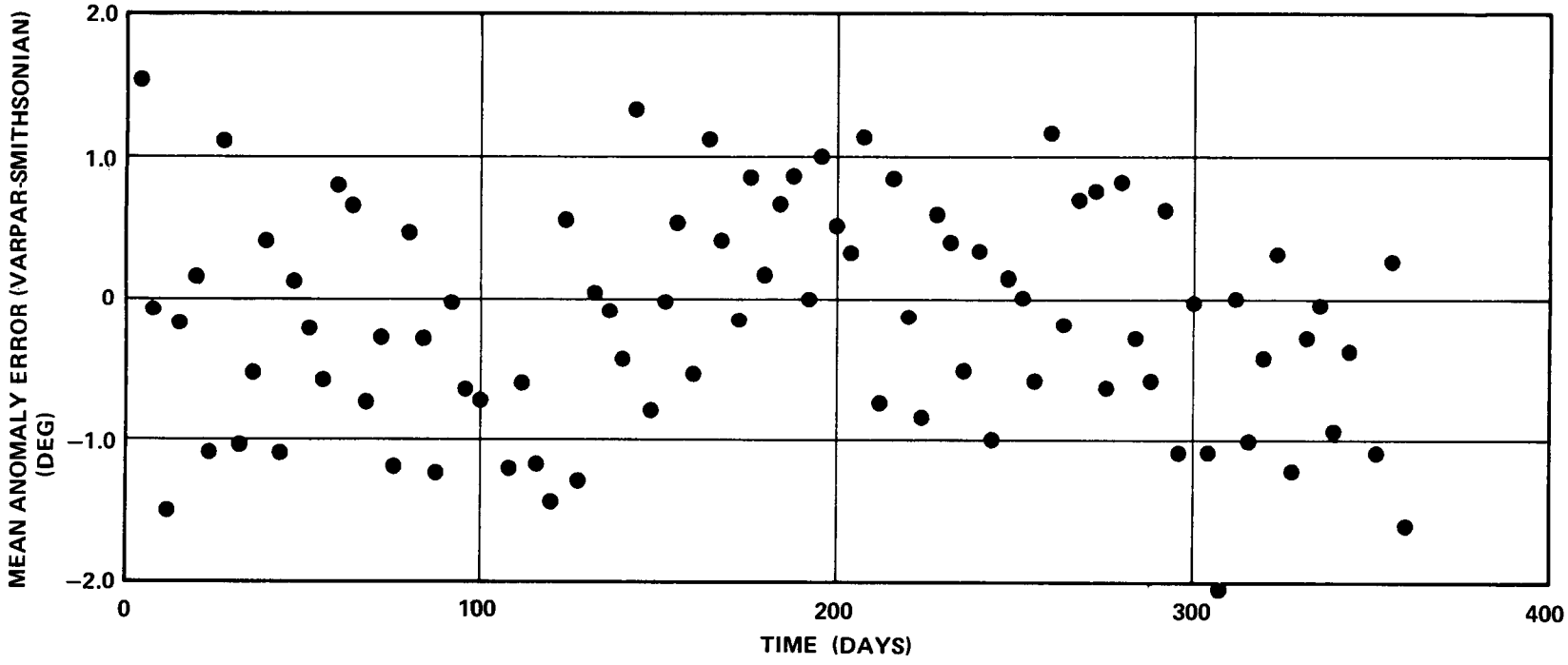


FIGURE 1 - THE ERROR IN MEAN ANOMALY FOR THE 1962 $\beta\mu$ SATELLITE

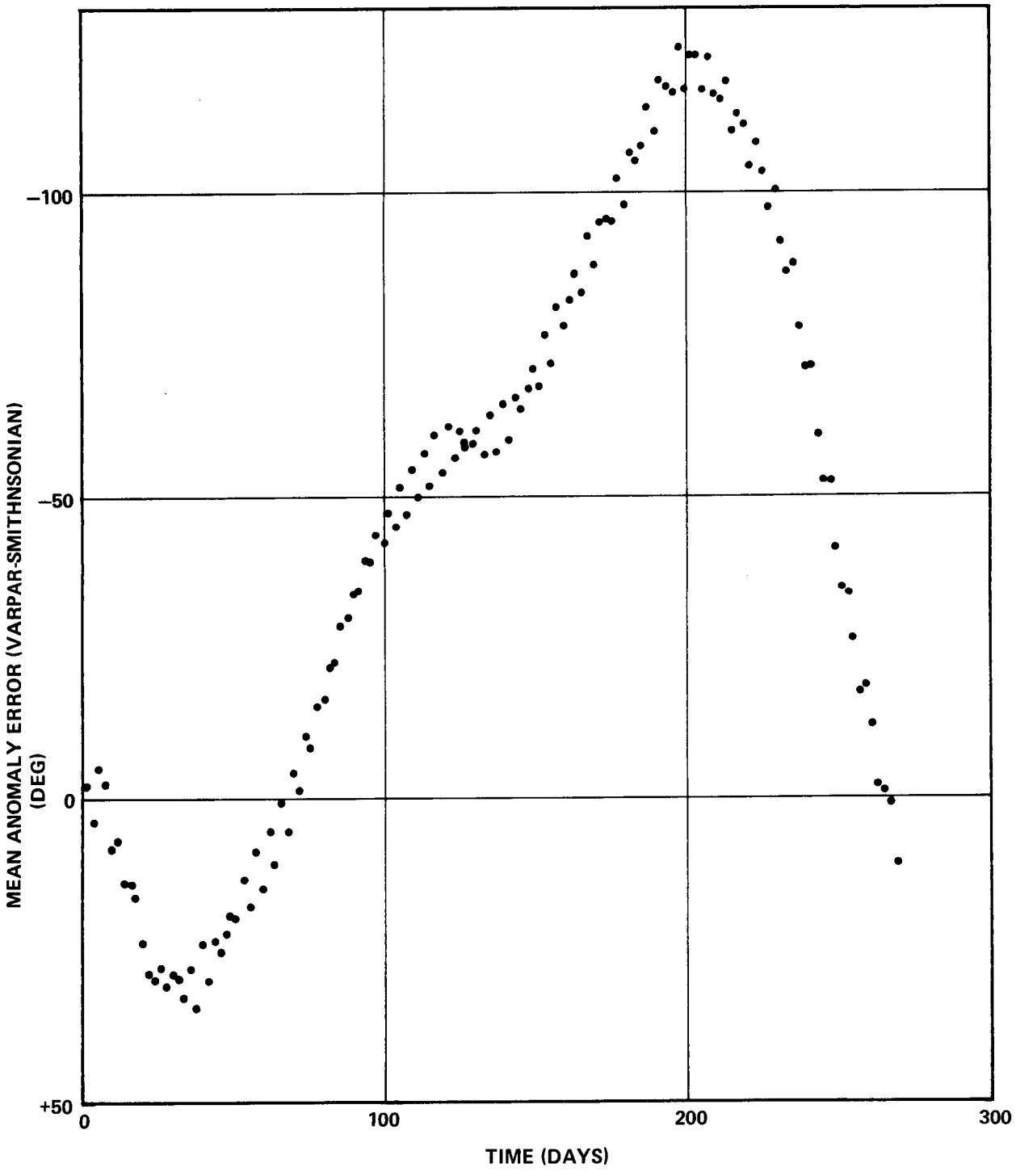


FIGURE 2 - THE ERROR IN MEAN ANOMALY FOR THE 1964-5A SATELLITE

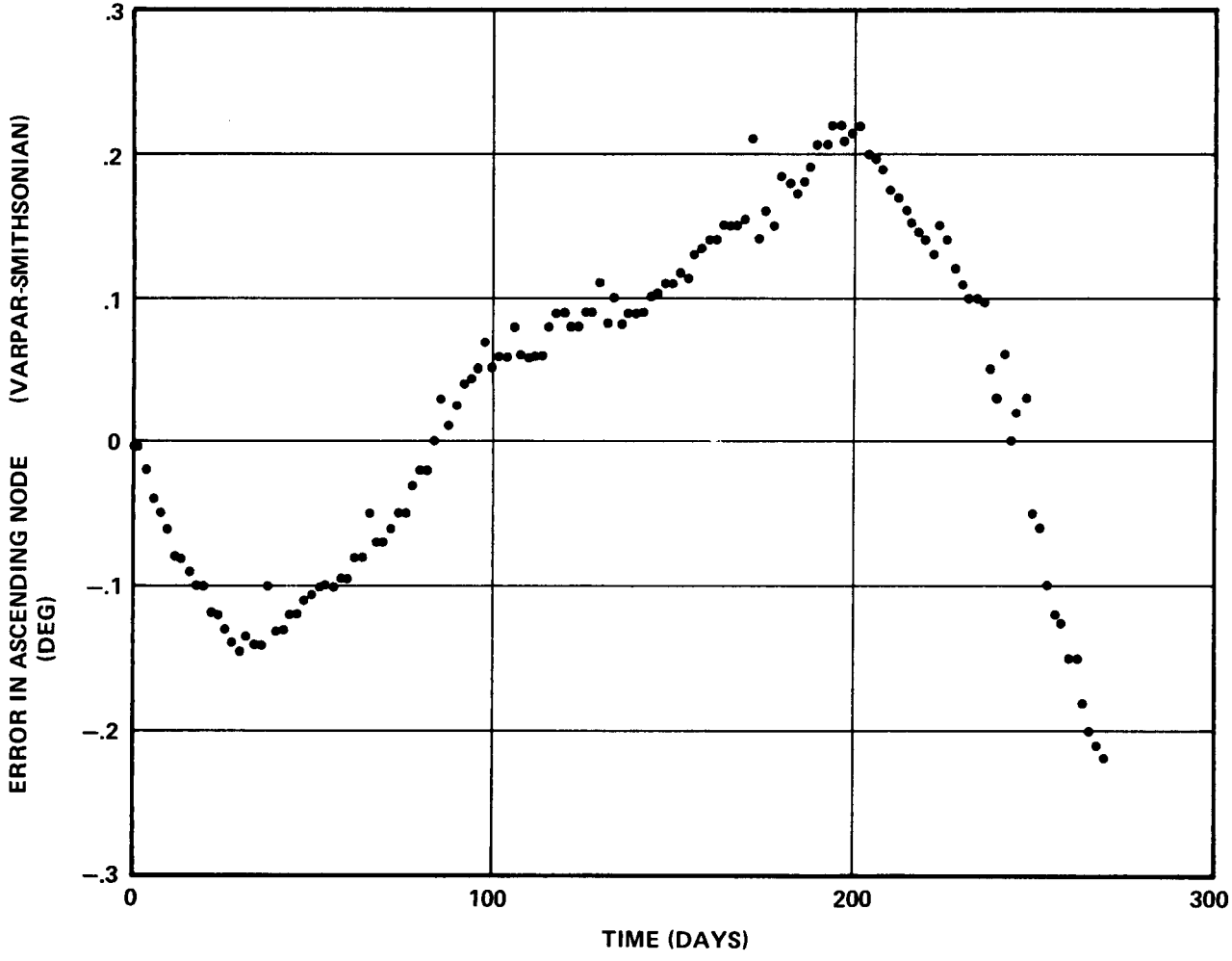


FIGURE 3 - THE ERROR IN RIGHT ASCENSION OF ASCENDING NODE FOR THE 1964-5A SATELLITE

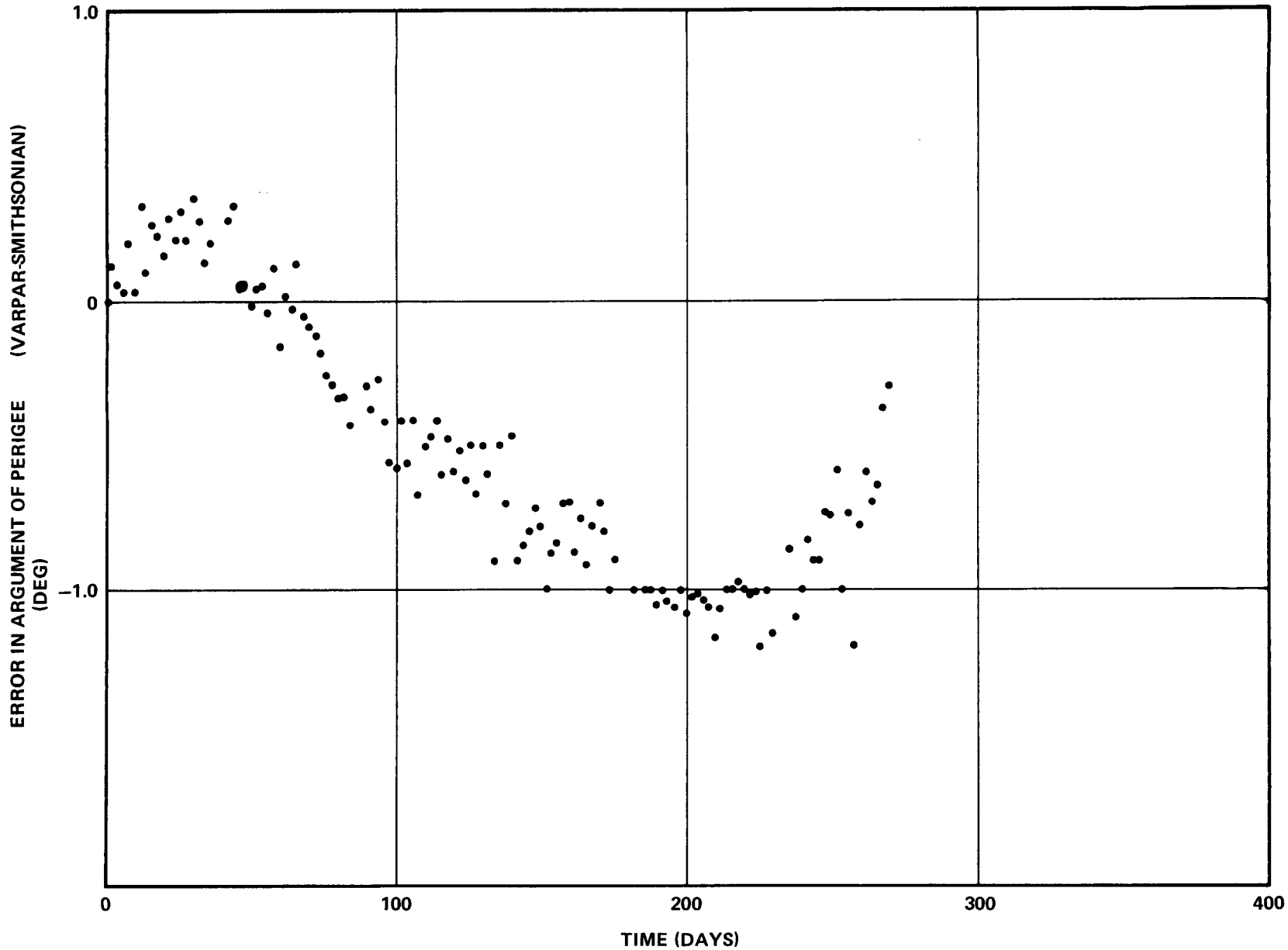


FIGURE 4 - THE ERROR IN THE ARGUMENT OF PERIGEE FOR THE 1964-5A SATELLITE

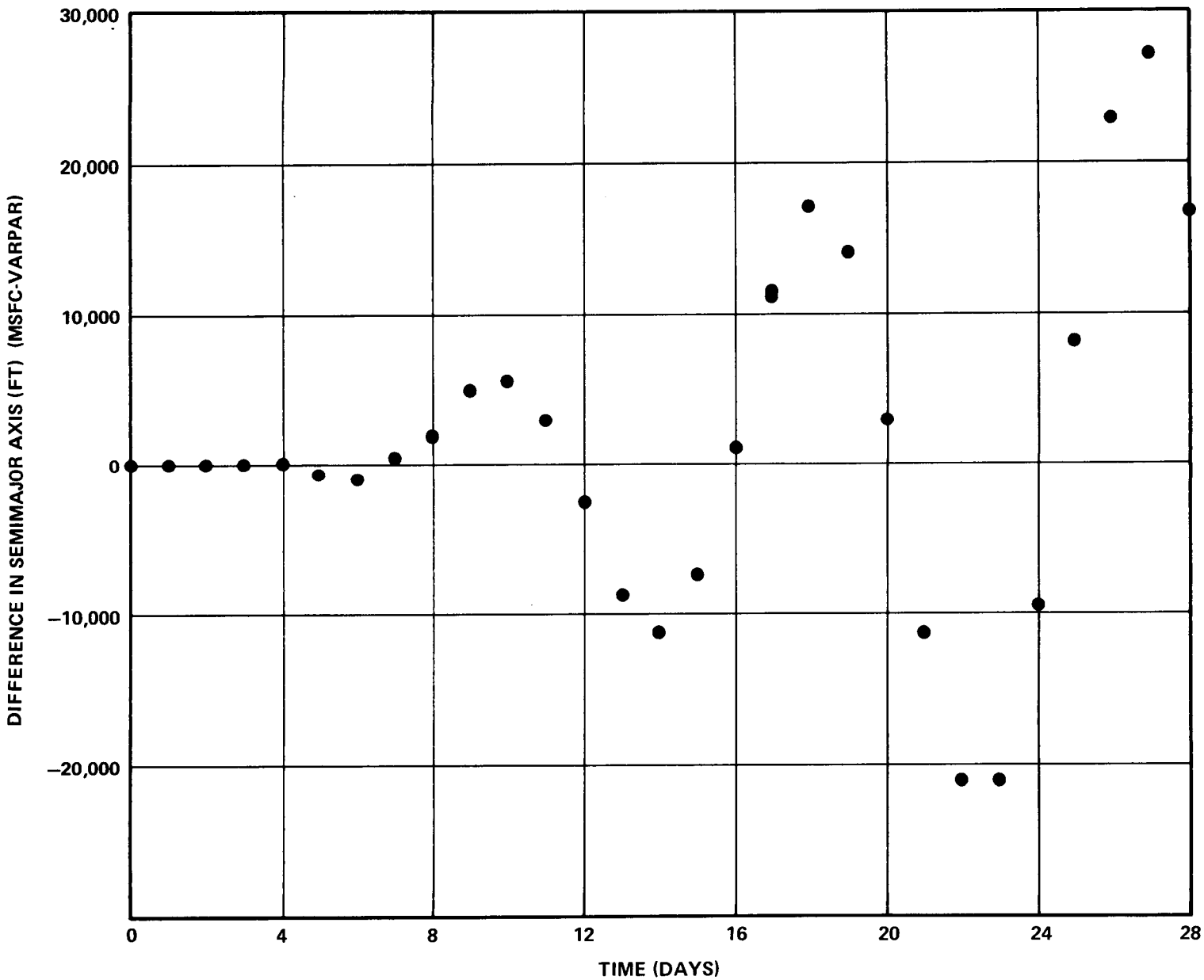


FIGURE 5 - THE DIFFERENCE IN SEMIMAJOR AXIS BETWEEN THE MSFC TRAJECTORY AND VARPAR

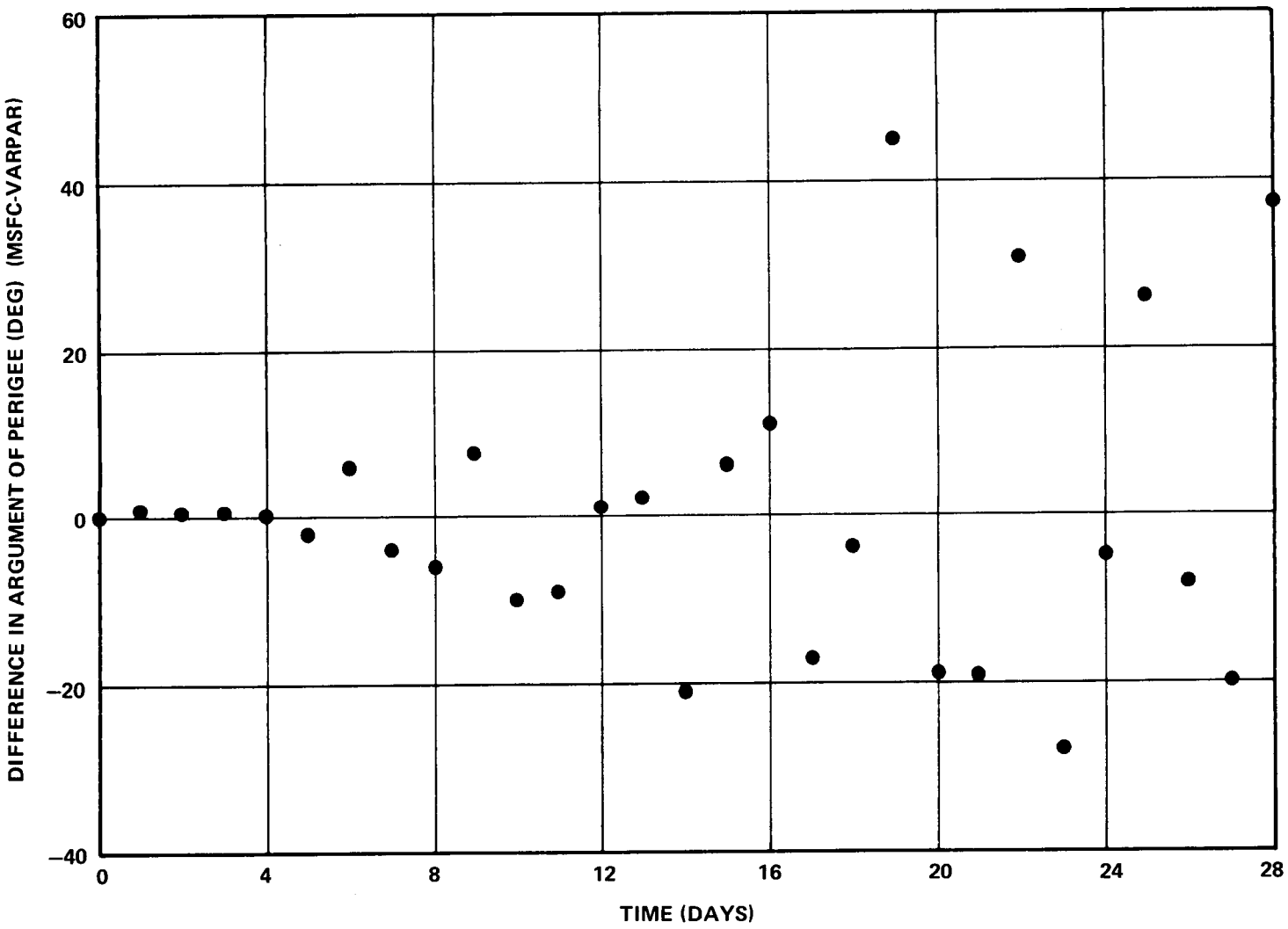


FIGURE 6 - THE DIFFERENCE IN ARGUMENT OF PERIGEE BETWEEN THE MSFC TRAJECTORY AND VARPAR

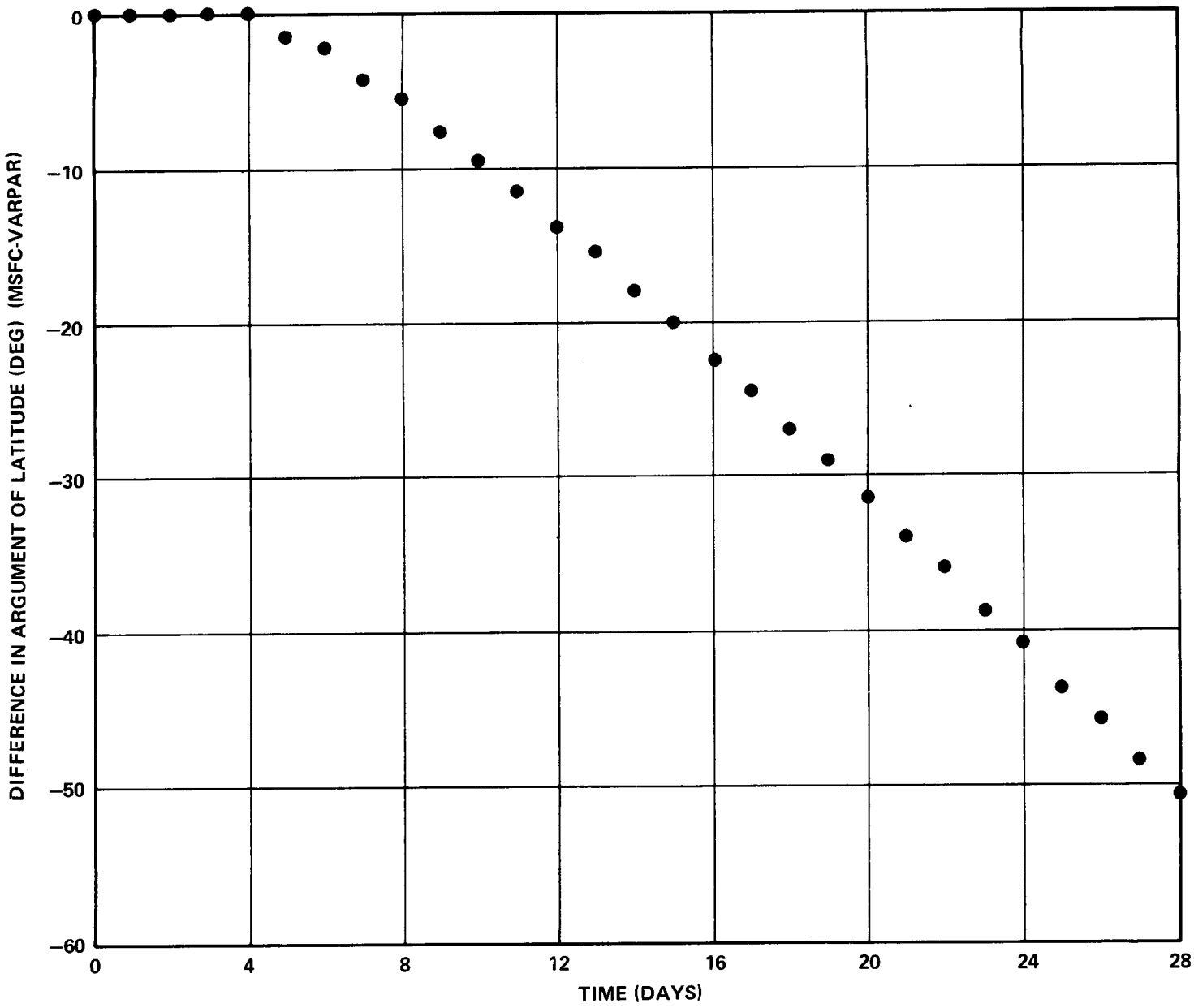


FIGURE 7 - THE DIFFERENCE IN ARGUMENT OF LATITUDE BETWEEN THE MSFC TRAJECTORY AND VARPAR

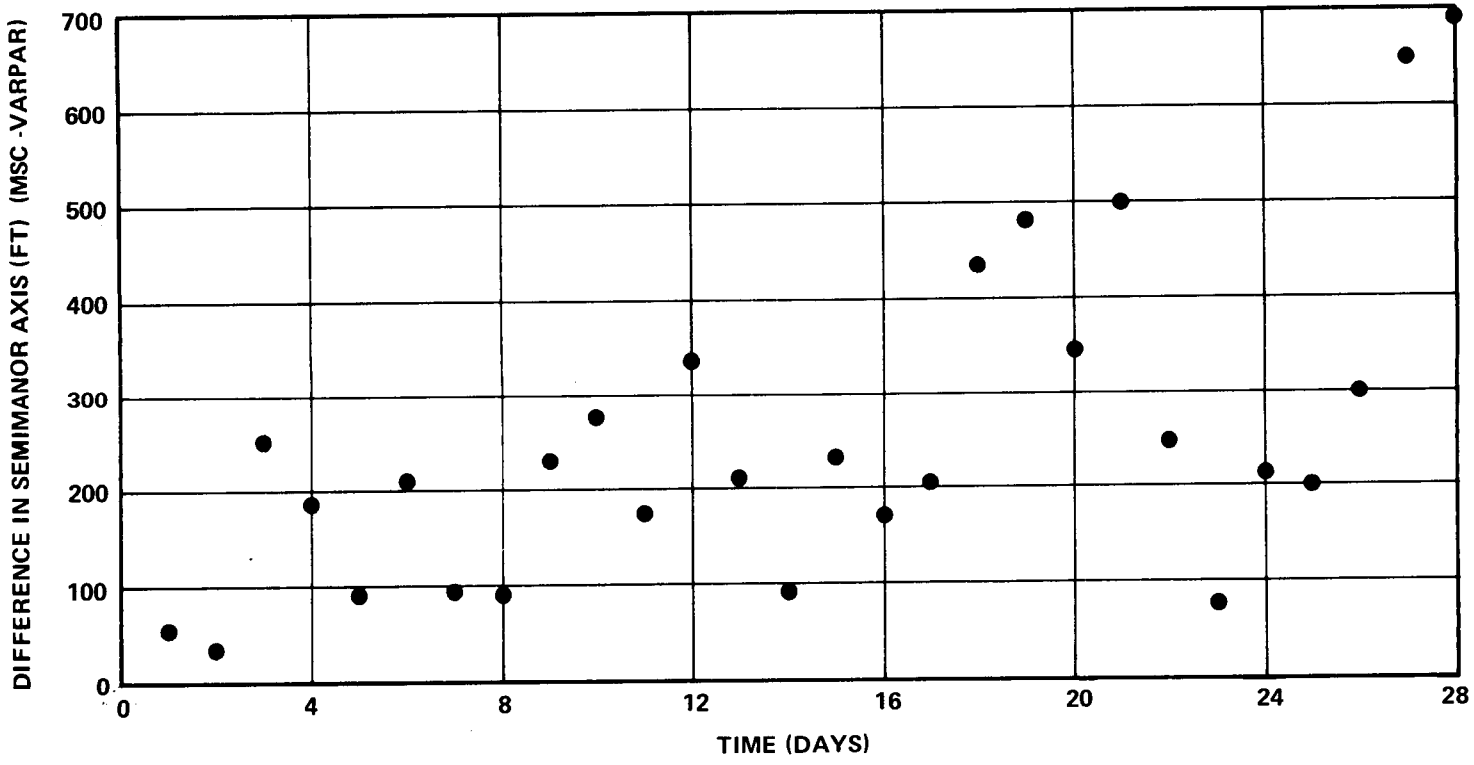


FIGURE 8 - THE DIFFERENCE IN SEMIMAJOR AXIS BETWEEN THE MSC TRAJECTORY AND VARPAR

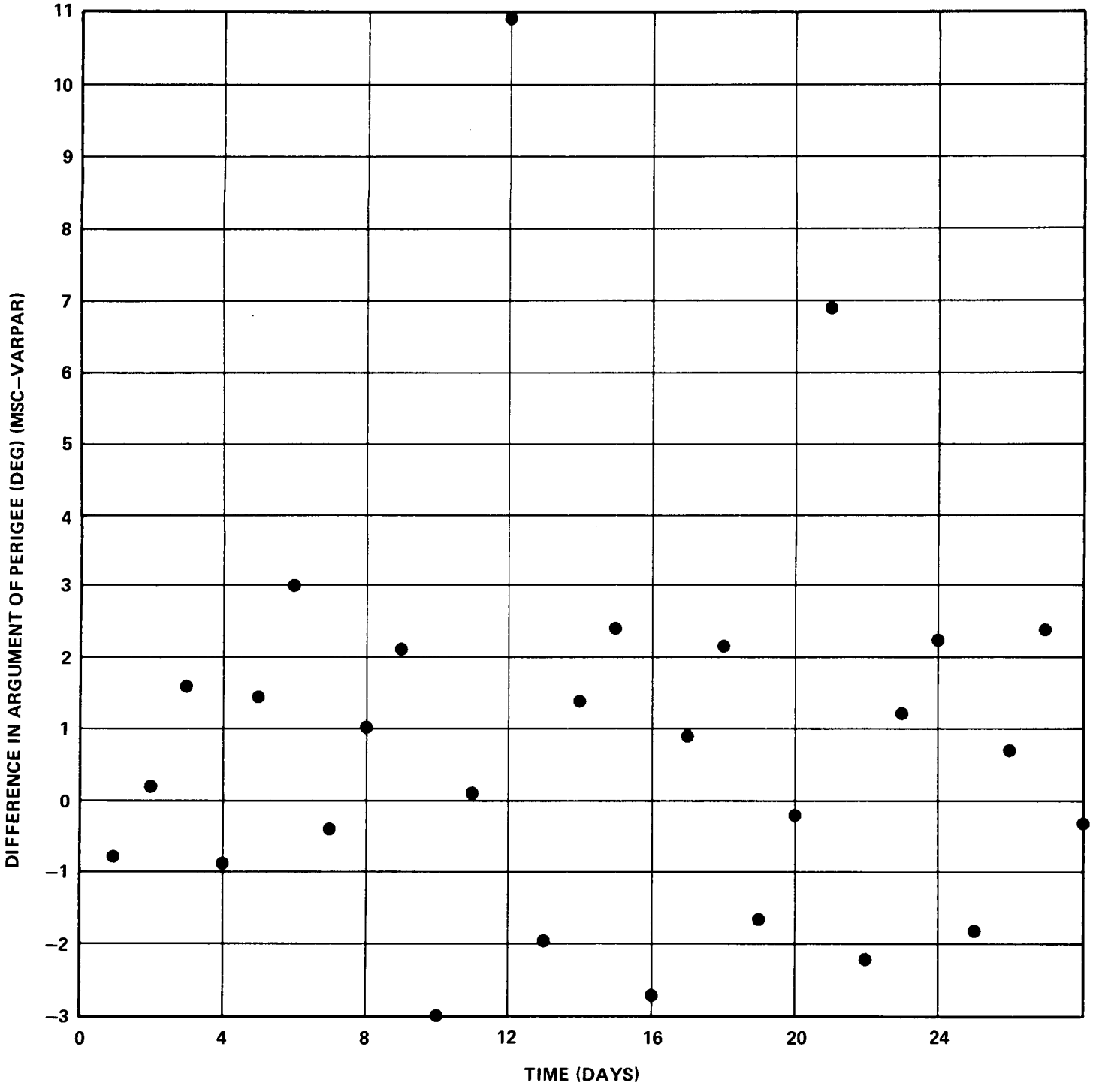


FIGURE 9 - THE DIFFERENCE IN ARGUMENT OF PERIGEE BETWEEN THE MSC TRAJECTORY AND VARPAR

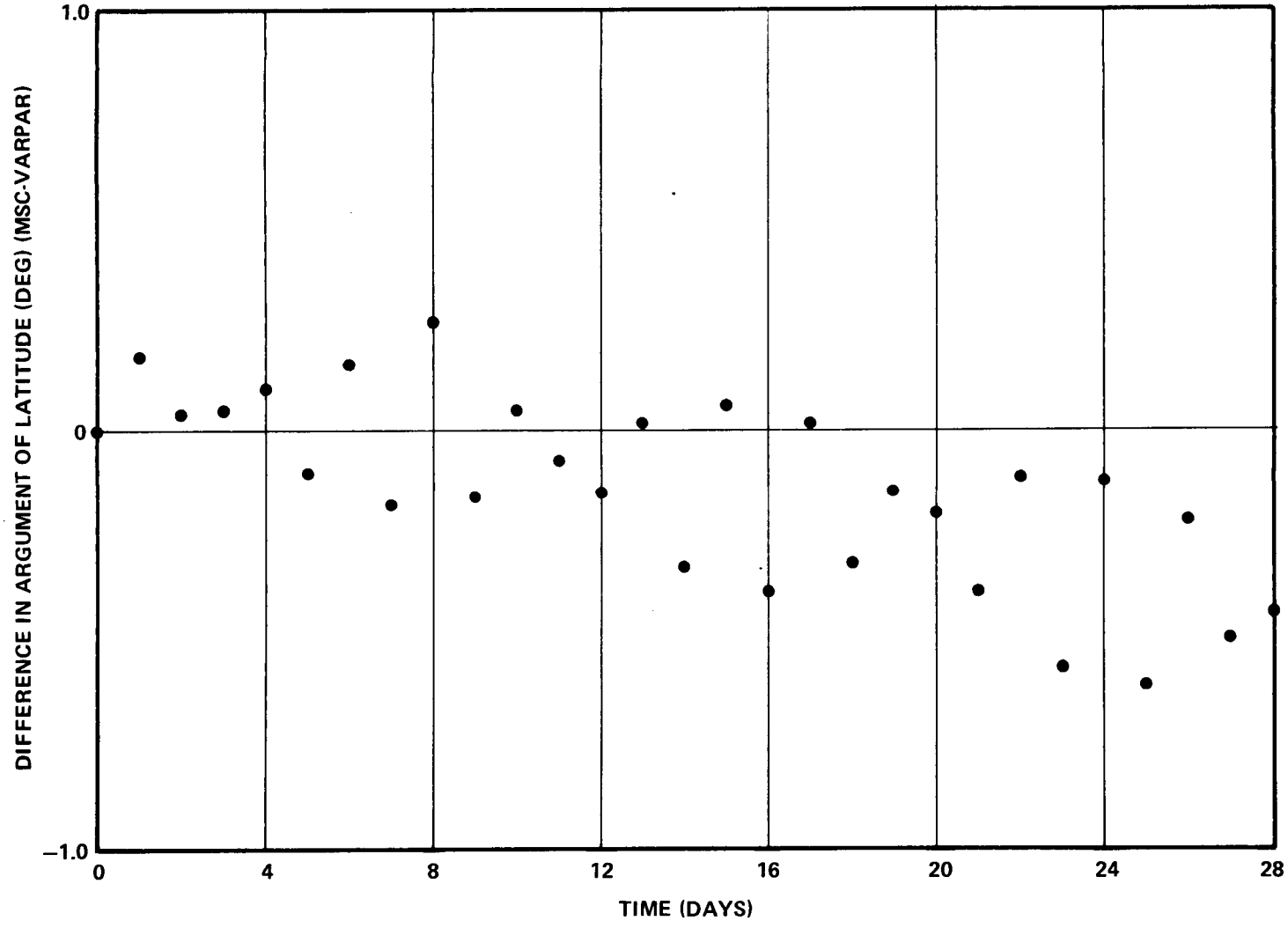


FIGURE 10 - THE DIFFERENCE IN ARGUMENT OF LATITUDE BETWEEN THE MSC TRAJECTORY AND VARPAR

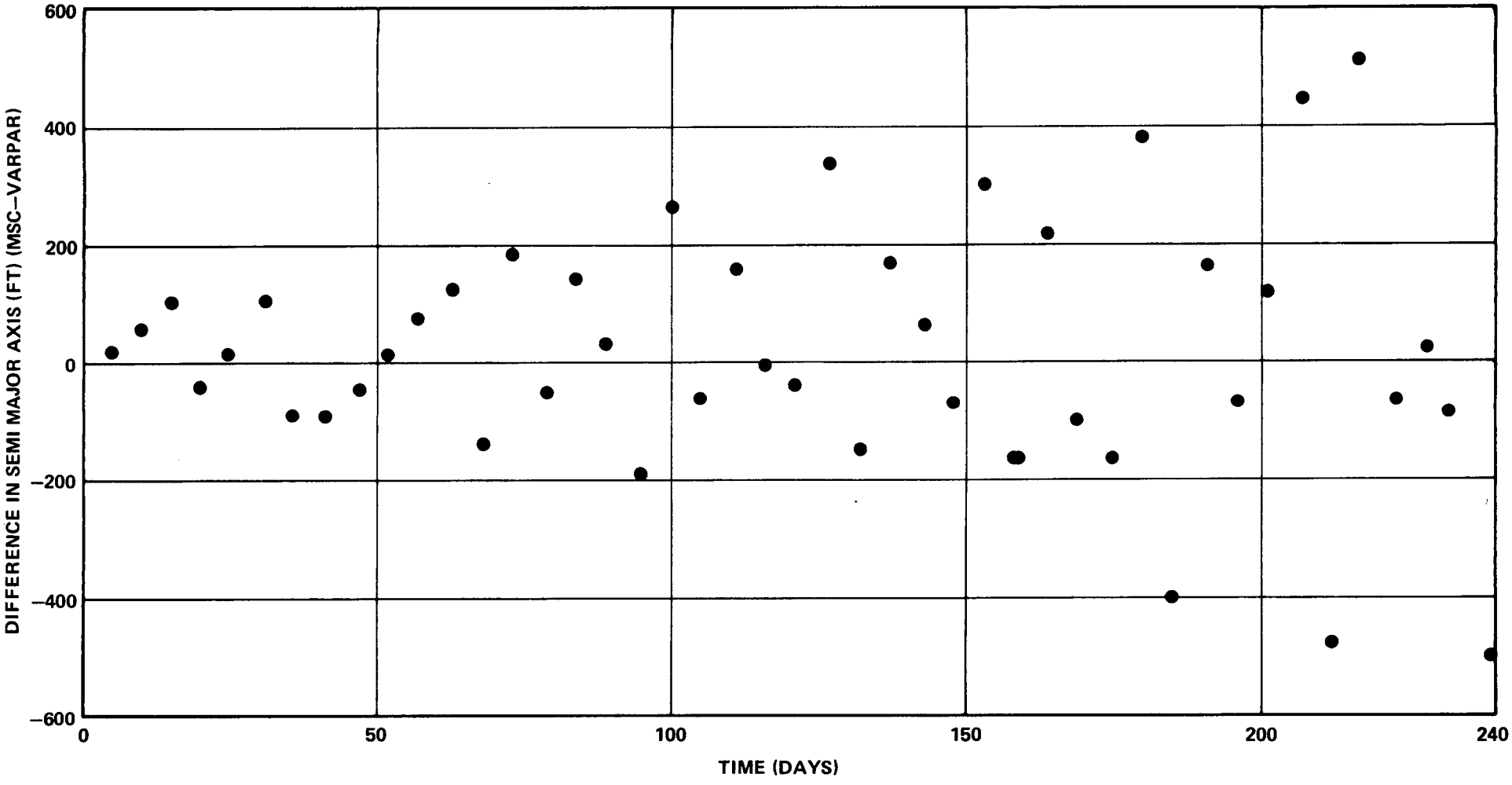


FIGURE 11 - THE DIFFERENCE IN SEMI MAJOR AXIS BETWEEN THE MSC TRAJECTORY AND VARPAR WITH NO DRAG PERTURBATIONS

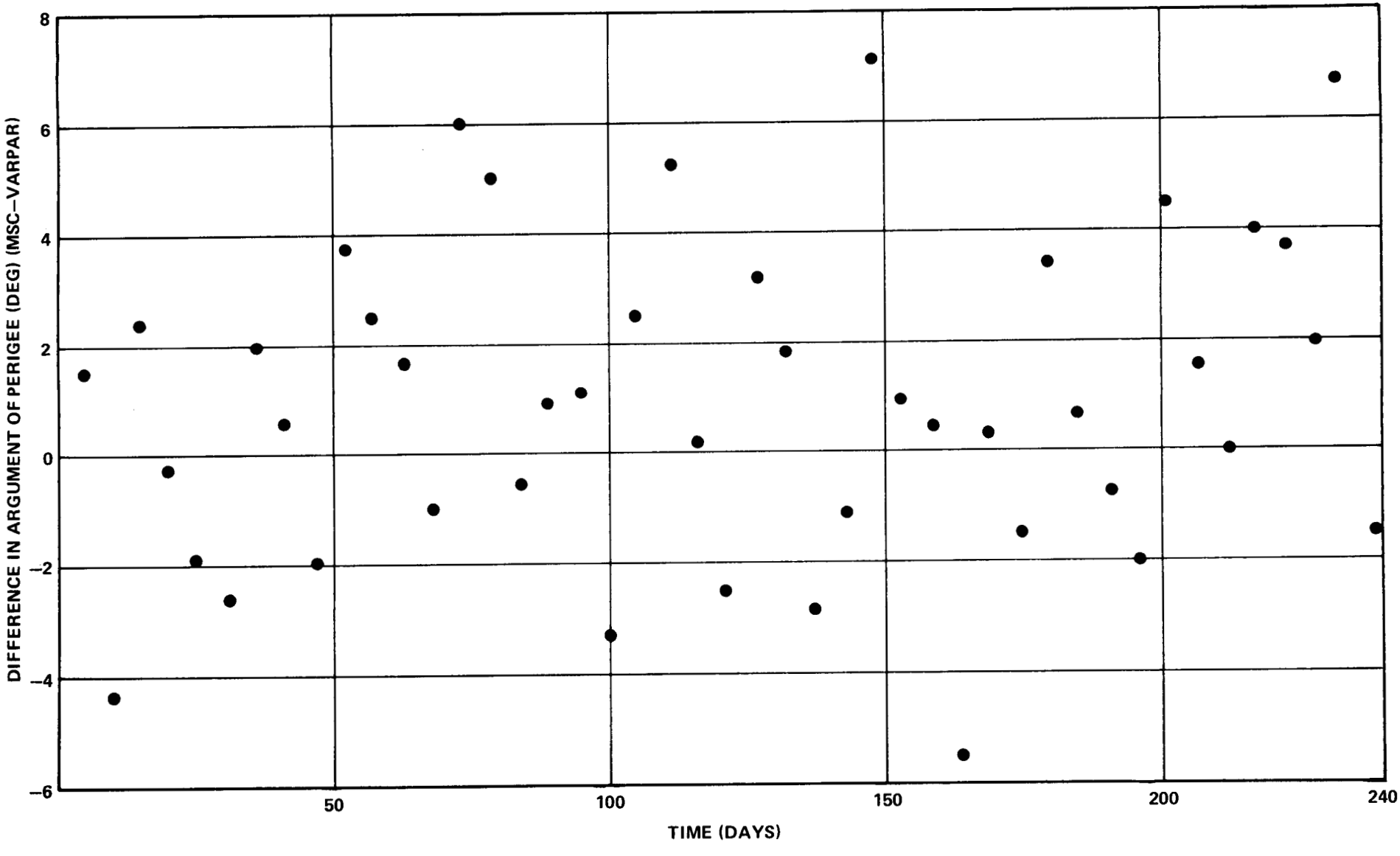


FIGURE 12 - THE DIFFERENCE IN ARGUMENT OF PERIGEE BETWEEN THE MSC TRAJECTORY AND VARPAR WITH NO DRAG PERTURBATIONS

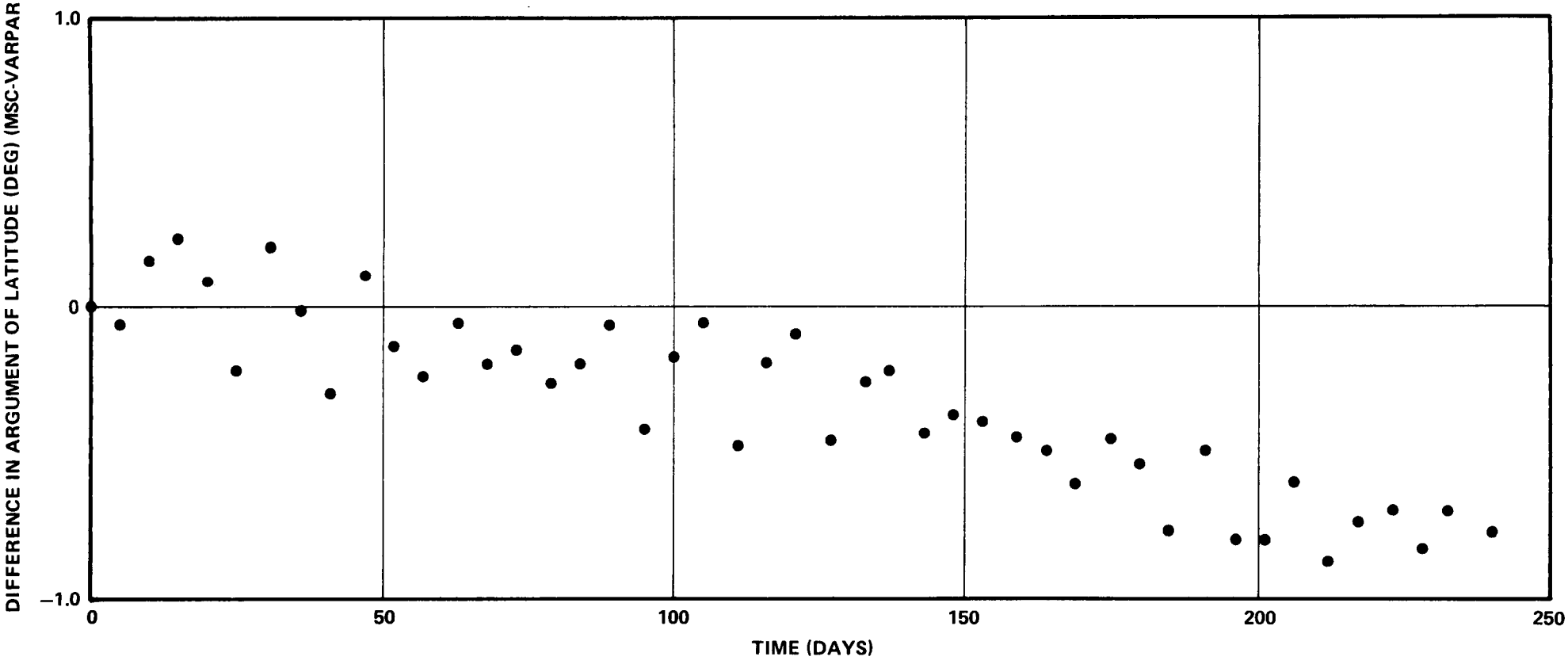


FIGURE 13 - THE DIFFERENCE IN ARGUMENT OF LATITUDE BETWEEN THE MSC TRAJECTORY AND VARPAR WITH NO DRAG PERTURBATIONS